



Effect of Pin Geometry and Tool Rotational Speed on Microstructure and Mechanical Properties of Friction Stir Spot Welded Joints in AA2024-O Aluminum Alloy

Tiwan^{a,b}, M. N. Ilman^{*a}, Kusmono^a

^a Department of Mechanical and Industrial Engineering, Faculty of Engineering, Universitas Gadjah Mada, Yogyakarta, Indonesia

^b Department of Mechanical Engineering Education, Yogyakarta State University, Indonesia

PAPER INFO

Paper history:

Received 24 April 2021

Received in revised form 19 May 2021

Accepted 01 July 2021

Keywords:

Friction Stir Spot Welding

AA2024-O Aluminum Alloy

Pin Geometry

Tool Rotational Speed

Shear Strength

ABSTRACT

In the present study, the effects of pin geometry and tool rotational speed on the microstructure and mechanical characteristics of the AA2024-O friction stir spot welding (FSSW) joint were investigated. Two different types of pin geometries, namely cylindrical and step pins, and three different rotational speeds of 900, 1400, and 1800 rpm were used in the friction stir spot welding joint. The microstructure observation, hardness measurements, and shear tests were conducted. Results showed that both pin geometry and rotational speed gave a remarkable effect on the microstructure and maximum shear load of the weld joints. For both pin geometries, the hook height and width of the fully bonded region (FBR) increased by increasing the rotational speed. The weld joint produced by a cylindrical pin exhibits higher values in the hook height and width of the FBR than using a step pin. Furthermore, the highest value in a maximum shear load was obtained at a rotation speed of 1400 rpm for both cylindrical and step pins. Another finding is that the maximum shear loads of FSSW joints produced with a cylindrical pin are higher than that made using a step pin.

doi: 10.5829/ije.2021.34.08b.16

1. INTRODUCTION

The application of aluminum alloys in automotive industries is mainly intended to produce lightweight vehicles which leads to fuel savings, high speed, and a reduction in exhaust emission. Today, aluminum and its alloys are produced in various series and treatments. One of the aluminum alloys that is widely used in engineering applications, especially for aircraft structures is AA2024 aluminum alloy which is composed of copper (Cu) around 3.8-4.9 wt% as the main alloying element. This aluminum alloy has the potency to replace steel in the manufacture of the vehicle body. In general, AA2024 aluminum alloy is used in the aircraft industry due to its beneficial properties, i.e. the alloy has high strength at room temperature to high temperature up to 150 °C and good toughness [1]. In addition, it has a very good damage tolerance and high fatigue crack resistance [2] which is suitable for aircraft materials.

Apart from its excellent properties, AA2024 aluminum alloy together with its 2XXX series are, however, considered to be unweldable [3] so that AA2024 aluminum alloy is commonly fabricated by riveting. The invention of friction stir welding (FSW) at The Welding Institute (TWI), UK in 1991 followed by its variant, i.e. friction stir spot welding (FSSW) allows the unweldable materials such as AA2024 to be welded using these solid-state welding processes [4-6]. The FSSW process has similarities with FSW in which both of them use a rotating cylindrical tool equipped with a shoulder and a pin to produce weld joints but they are different in term of the tool movement that is the rotating tool in FSW moves along a weld line in the butt plane of the plates whilst the rotating tool in FSSW is operated in a stationary condition [7]. FSSW is performed by plunging the rotating tool into the sheets in the lap joint configuration. The heat generated by frictional forces leads to softening in the materials to be welded. As a

*Corresponding Author Institutional Email: ilman_noer@ugm.ac.id
(M. N. Ilman)

result, the softened materials of upper and lower sheets are mixed due to stirring action by the pin, and under such a condition, the weld joint is formed.

Since the invention of FSSW by Mazda's car manufacturer in 2003 [8], research in FSSW has been conducted extensively to improve mechanical characteristics of FSSW joints by considering factors affecting the mechanical properties of FSSW joints including process parameters and tool geometry in various metals. The influence of shoulder and pin geometries of a tool on the microstructure and mechanical characteristics of the FSSW joint in AA2024-T3 aluminum alloy has been studied by Paidar et al. [9]. According to the authors, at a low tool rotational speed, the grain size in the stirring zone is influenced by the pin geometry while at a high tool rotational speed, there is no significant difference in the grain size. Badarinarayan et al. [10] showed that the shape of the tool pin affects the hook, weld strength, and failure mode of the FSSW joint. Enami et al. [11] investigated the influences of welding parameters (plunge depth, dwell time, and tool rotational speed) and addition of alumina nanopowder on the FSSW joint strength and found that the normal plunge depth, dwell time, and tool rotational speed effectively affect the joint strength of AA2024 alloy. In addition, the optimum welding parameters are achieved at a speed of 1120 rpm, 5s dwell time, and normal plunge depth of 2.75, and the joint strength increased by 23% by the addition of alumina nanopowder. Subsequently, Klobčar et al. [12] have investigated the effect of process parameters on the strength of AA5754 FSSW joint with the results showed that axial force and torque increased with increasing plunge rate but they decreased with increasing dwell time and tool rotation speed. Other FSSW process parameters such as plunge depth have been investigated by Baek et al. [13] and according to the authors, plunge depth affects the shear strength of the FSSW galvanized steel joint. The effects of both plunge rate and dwell time on the joint strength of AA1100 sheets under micro FSSW were studied by Baskoro et al. [14]. They found that the dwell time gives a remarkable effect on the tensile shear strength but the plunge rate has a minor effect. Other studies on the effect of FSSW process parameters on the shear strength of FSSW joint have been conducted to optimize FSSW process parameters to produce the high quality of the joints [15-18]. Recently, Tiwan et al. [19] studied the effects of pin geometry and rotational speed on the microstructure and mechanical characteristics of the AA5052-H112 FSSW joint. They found that both pin geometry and rotational speed have a significant effect on the hook height and width of FBR of the FSSW joints. Moreover, the strength of the weld joints produced by a cylindrical pin is higher than that of a step pin. The effect of tool rotating speed (700, 900, and 1100 rpm) on the microstructures and mechanical characteristics of the AA6061 FSSW joints welded in air and water was also

demonstrated by Shekhawat et al. [20]. They found that the load-bearing capacity improved and also a slight increase in hardness when the rotational speed increases from 700 to 1100 rpm, irrespective of the welding medium. This increase is attributed to the grain size refinement in the weld nugget zone. In addition, the FSSW in water is obtained to be beneficial as compared to that in air.

The quality characteristics of FSSW joints formed in the metal alloy are strongly influenced by design and welding parameters. One of the most important factors influencing the quality of the FSSW joints is the design of the tool used for producing the friction and stirring action [21]. It seems that research works related to the FSSW in AA2xxx series aluminum alloys have been studied extensively, but there have been limited published data on the influences of pin geometry and rotational speed on the microstructure and strength of the FSSW AA2024-O aluminum alloy joints. Therefore, it is the subject of the present work. Two different types of pin geometries, i.e., cylindrical and step pins, and three different rotational speeds of 900, 1400, and 1800 rpm were selected for the AA2024-O FSSW joint.

2. MATERIAL AND EXPERIMENTAL

The materials used in this work were AA2024-O aluminum alloy plates with the chemical composition is given in Table 1. In this investigation, the plates with the dimension of 3 x 30 x 120 mm were welded using the FSSW process in lap joint configuration. The plates to be welded were tightly clamped using a jig. The tools having two different tool pin geometries, namely cylindrical and step pins were made of H13 steel as shown in Figure 1. The FSSW joints were produced using various tool rotational speeds (RS) of 900 rpm, 1400 rpm, 1800 rpm whereas other FSSW parameters including plunge depth, plunge rate, and dwell time were maintained constant at 0.1 mm, 4 mm/min and 5s, respectively.

The temperatures during welding were measured using K-type thermocouples attached at various distances of 0, 4, 5, 6, 7, 8 mm from the center of the weld hole as shown in Figure 2. Microstructure examinations were performed on the cross-section of the FSSW joints using optical microscopy. The samples were prepared

TABLE 1. Chemical compositions of AA2024-O aluminum alloy

Chemical composition (wt.%)								
Cu	Mg	Si	Fe	Zn	Ti	Mn	Cr	Al
4.4	1.11	0.12	0.14	0.08	0.01	0.40	0.01	Bal.

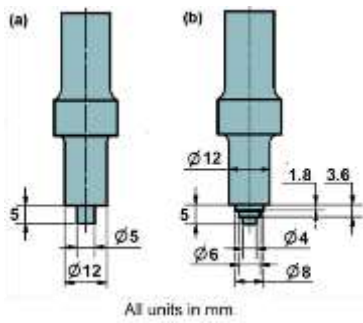


Figure 1. FSSW tools type:(a) Cylindrical pin (b) Step pin

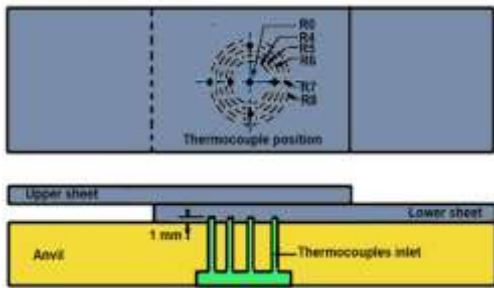


Figure 2. A schematic illustration of the FSSW process

following standard metallographic procedures with etchant used was Keller's reagent.

Furthermore, hardness distributions were assessed using Vickers microhardness along with the upper and lower plates around the FSSW joints as shown in Figure 3 with the load of 100 g for 10 s. The strength of FSSW joints was assessed using shear tests with the dimensions of shear test specimens are presented in Figure 4 as suggested by Kim et al. [22]. Following these shear tests, fractographic studies were conducted.

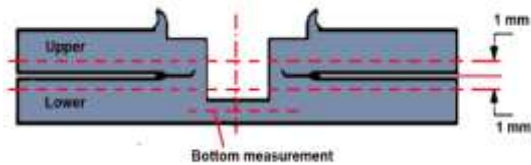


Figure 3. Position of hardness measurement

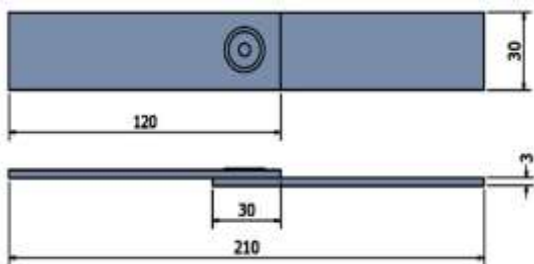


Figure 4. Tensile-shear test specimens

3. RESULT AND DISCUSSION

3. 1. Weld Thermal Cycles

The thermal cycles taken at various distances of 0, 4, 5, 6, 7, and 8 mm from the center of the exit hole (designated as R0, R4, R5, R6, R7 and R8, respectively) during friction stir spot welding (FSSW) of AA2024-O aluminum alloy plates at two different tool pin geometries are demonstrated in Figures 5 and 6.

Referring to Figures 5 and 6, it can be seen that each thermal cycle under study shows similar behaviors marked by rapid heating as the shoulder surface penetrates the workpiece. Furthermore, the maximum temperature is achieved when the distance between the tool tip and the bottom surface of the lower plate is

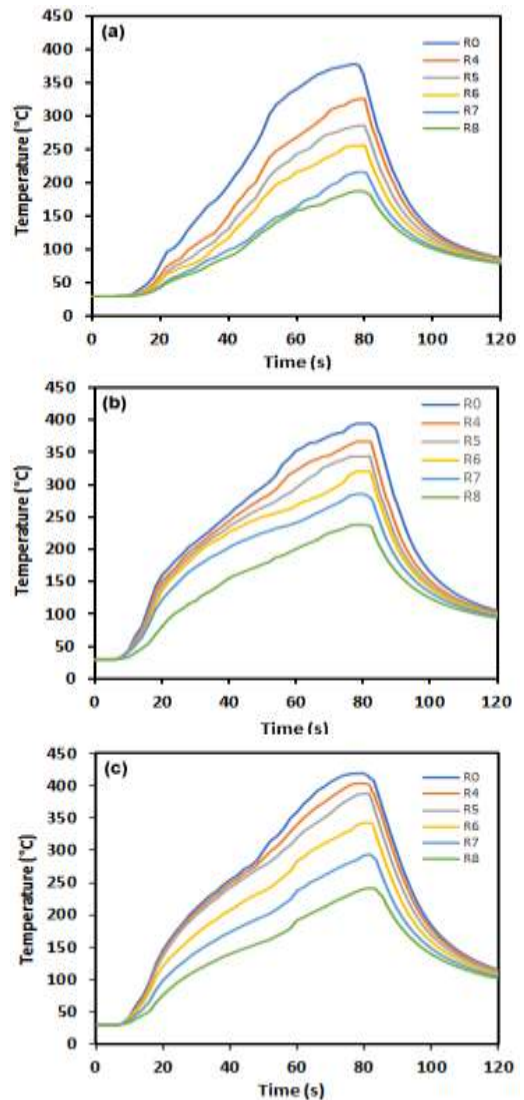


Figure 5. Thermal cycles of FSSW AA2024 using a cylindrical pin with variation in RS: (a) 900 rpm (b) 1400 rpm (c) 1800 rpm

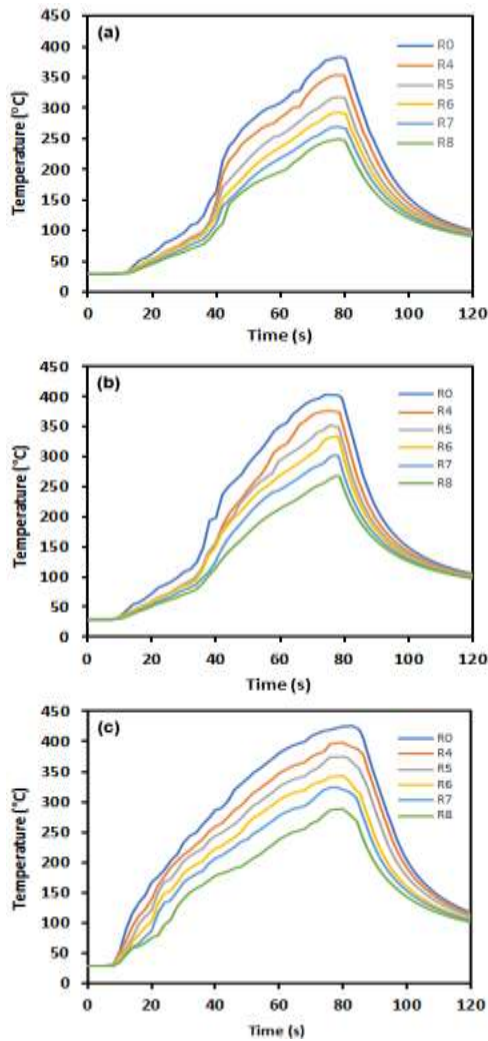


Figure 6. Thermal cycles of FSSW AA2024 using a step pin with variation in RS: (a) 900 rpm (b) 1400 rpm (c) 1800 rpm

the closest, typically 0.1 mm. At this condition, the maximum temperature is maintained constant for 5s then followed by continuous cooling towards the ambient temperature as the tool is lifted. Referring to Figures 5 and 6, it can be seen that increasing distance from the center of the keyhole decreases the peak temperature and the position of the peak temperature is shifted to a slightly longer time. Of note is that the peak temperatures resulted by cylindrical and step at the distance of R0 are slightly the same but as the distance, the significant differences are observed with the peak temperatures resulted from step pin is higher than that of cylindrical pin.

This seems to suggest that FSSW having a step pin produces higher heat input than that of the cylindrical pin at the same tool rotational speed.

The effects of tool rotational speed on the weld thermal cycles can be studied by comparing the welds made at the tool rotational speeds of 900, 1400, and 1800

rpm for both cylindrical and step pins. As expected, an increase in tool rotational speed tends to increase the peak temperature and reduce the cooling rate. In comparison with the tool having cylindrical pin geometry, the peak temperatures for the FSSW joints produced using step pin are slightly higher at the same tool rotational speed. The possible explanation is summarized as follows. The heat generated, q by a conventional tool having a cylindrical pin is given by following expression [23, 24]:

$$q = \frac{2}{3} \pi \omega \tau (R_{shoul}^3 + 3R_{pin}^2 H_{pin}) \tag{1}$$

With τ is shear stress, ω is angular speed, H_{pin} is pin height whereas R_{pin} and R_{shoul} are the radius of pin and shoulder respectively. According to Equation (1), the use of a step pin will increase the shoulder area hence increasing the heat since the shoulder has more contribution to the total heat compared to other components such as pin side and pin tip.

3. 2. Macro and Microstructures

Figure 7 shows typical macrostructural regions taken from a cross-section of FSSW joint prepared using a tool having a cylindrical pin. The hole shown in Figure 7a is formed when the rotating tool was retracted from the weld joint. It can be seen that the FSSW profile is symmetrical concerning the hole-axis. There are three types of interface bonds, namely fully bonded region (FBR), partially bonded region (PBR), and unbonded region (UBR) [25]. The closest region to the exit hole is known as FBR which is marked by the presence of a perfect bond as the result of stirring of the upper and lower plate materials. Subsequently, PBR is formed starting from FBR to the distance where the bonding no longer exists. PBR has an imperfect bond which occurs caused by the lack of a diffusion process between the surface of the upper and lower plates. At the distance away from the hole exit, the upper and lower plates are separated with no bond formation, and this region is called UBR.

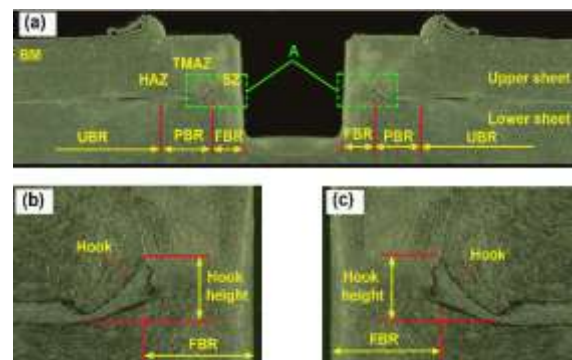


Figure 7. (a) Cross-section of FSSW joint, (b), (c) magnified region marked by A in Figure 6a showing various weld microstructures

Figures 8 and 9 show cross-sections of FSSW weld joints produced using a cylindrical pin and a step pin at various rotational speeds of 900 rpm, 1400 rpm, and 1800 rpm. It can be seen that all FSSW joints are characterized by the formation of hooks and microstructural regions with different dimensions. The hooks are formed when the interface is bent upward as the result of penetration and stirring of the tool which causes the bottom plate material to flow upward [26].

Details of the dimensions of FBR and the hooks under various tool rotational speeds at two different pin geometries are shown in Figures 10 and 11. In FSSW joints prepared using a cylindrical pin, the dimensions of the FBR increase with increasing rotational speed consistent with the previous report [25].

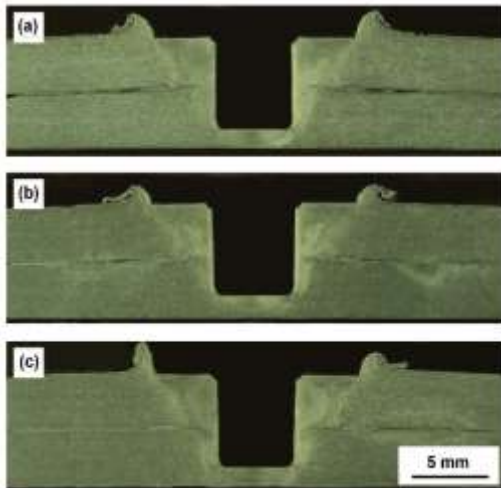


Figure 8. FSSW welded macrostructure by a cylindrical pin at RS: (a) 900 rpm, (b) 1400 rpm (c) 1800 rpm

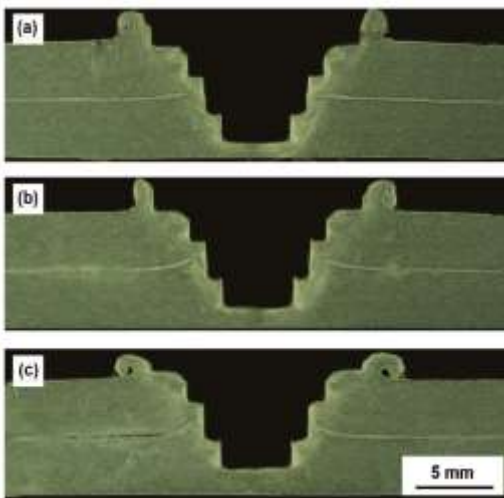


Figure 9. FSSW welded macrostructure by a step pin at RS: (a) 900 rpm, (b) 1400 rpm (c) 1800 rpm

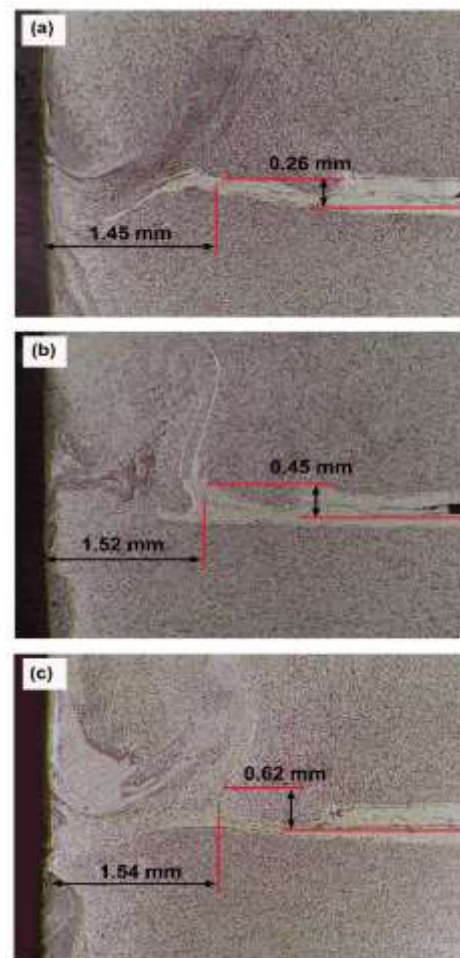


Figure 10. FBR dimension and height hook of FSSW by a cylindrical pin under different RS: (a) 900 rpm (b) 1400 rpm (c) 1800 rpm

The use of a rotational speed of 900 rpm produces FBR with a length of 1.45 mm. Subsequently, the length of FBR increases to 1.52 mm as the tool rotational speed is increased to 1400 rpm. On further increase in the tool rotational speed up to 1800 rpm, the dimension of FBR length continues to increase with the length of 1.54 mm. Similar behavior is also observed in the hook height. The hook height continuously increases from 0.26 mm to 0.45 mm and finally, 0.62 mm as the tool rotational speeds are increased to 900, 1400, and 1800 rpm, respectively.

In the step pin, there is a slight increase in the dimensions of the FBR from 1.31 mm to 1.33 mm as the tool rotational speed is increased from 900 to 1400 rpm. Further increase in the rotational speed to 1800 rpm does not increase the dimensions of FBR. Similar trends are observed in the hook heights under increasing tool rotational speeds marked by the hook heights of 0.23 mm, 0.25 mm, and 0.27 mm at increasing tool rotational speeds of 900, 1400, and 1800 rpm, respectively.

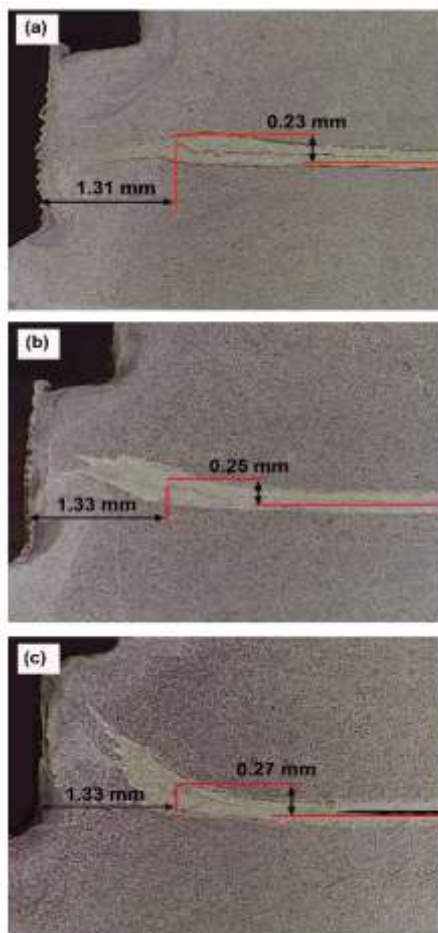


Figure 11. FBR dimension and height hook of FSSW by a step pin under different RS: (a) 900 rpm (b) 1400 rpm (c) 1800 rpm

Results of this investigation show that FBR dimensions (FBR length and hook height) of FSSW welds prepared using the step pin tool tend to be lower than the cylindrical pin which may be linked to material flow during welding. Based on the terminology used in FSSW [27, 28], microstructural regions in the FSSW can be classified into four regions, namely stir zone (SZ), thermomechanical affected zone (TMAZ), heat affected zone (HAZ), and base material (BM). Figures 12 and 13 show typical microstructures taken from various regions of FSSW joint produced using the tools having cylindrical and step pins at the tool rotational speed of 1400 rpm. The microstructure in SZ prepared using both cylindrical and step pins is characterized by the presence of fine equiaxed grains due to dynamic recrystallization of the material around the pins [29]. The microstructure of TMAZ has fine bent and deformed grains resulted from the combined effect of heat and plastic deformation [30].

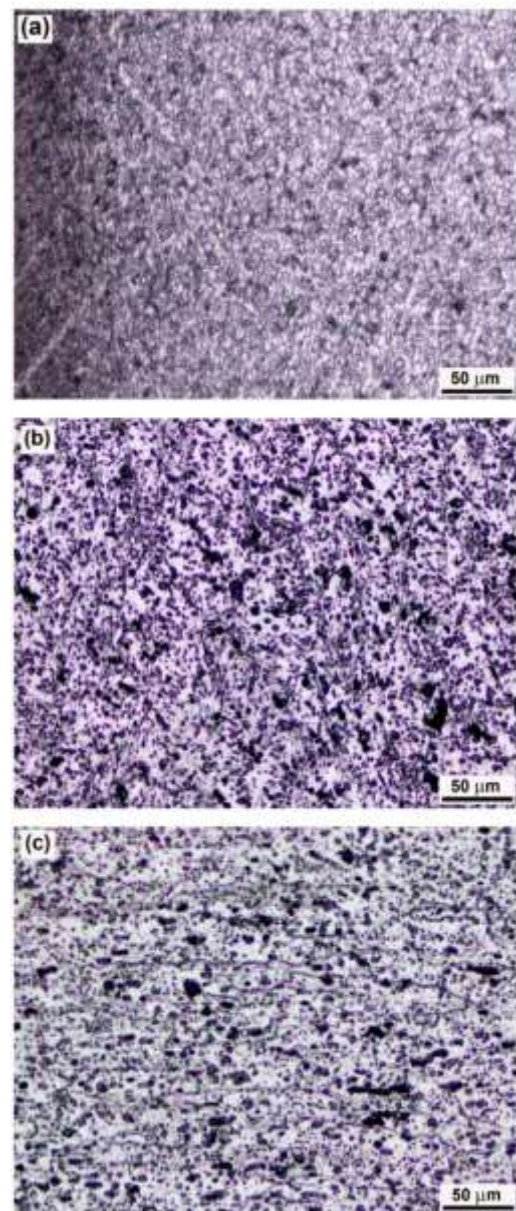


Figure 12. Microstructure of FSSW welded using a cylindrical pin at the RS of 1400 rpm: (a) SZ (b) TMAZ (c) HAZ

In HAZ regions, the microstructures are influenced by heat only and they are characterized by coarser polygonal grains [31]. In general, various microstructure present in both the welds prepared using the tools having cylindrical and step pins are the same but they are different in term of grain size with the tool equipped with step pin produces coarser microstructure.

Stir zone (SZ) microstructures of the FSSW joints produced using the cylindrical pin and step pin at various tool rotational speeds are presented in Figures 14

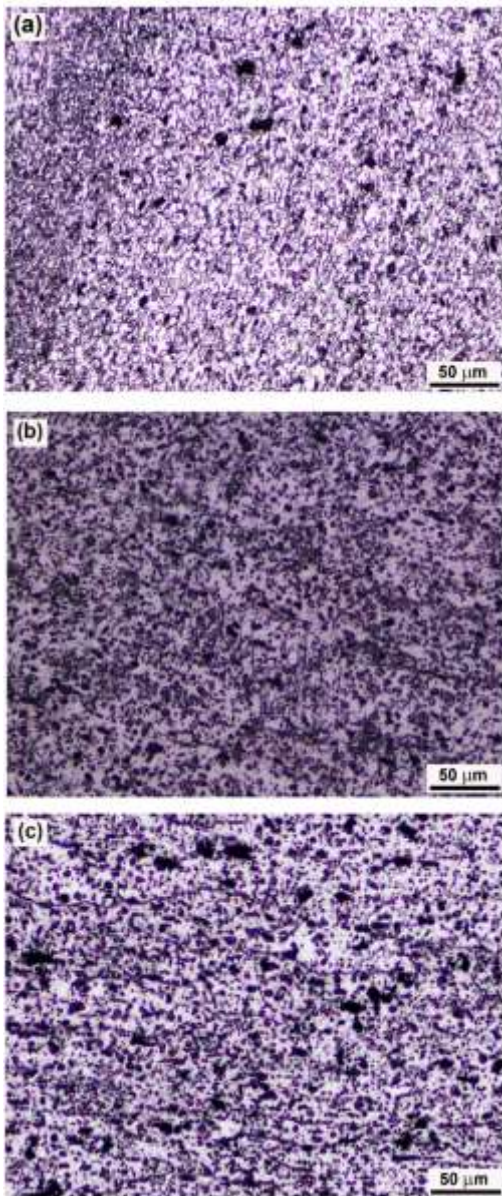


Figure 13. Microstructure of FSSW welded used a step pin at the RS of 1400 rpm: (a) SZ (b) TMAZ (c) HAZ

and 15. It can be seen that increasing tool rotational speed tends to grains coarsening the microstructures [32]. Referring to Figures 14 and 15, it can be seen the microstructures produced using the step pin are coarser than those produced using the cylindrical pin.

3. 3. Hardness Distributions

Results of microhardness measurements for all FSSW joints under study are shown in Figures 16 and 17.

It can be seen that the hardness profiles of all FSSW joints have the same behaviors, i.e. the maximum hardness occurs at the keyhole side for both upper and lower sheets which is likely to be associated with re-

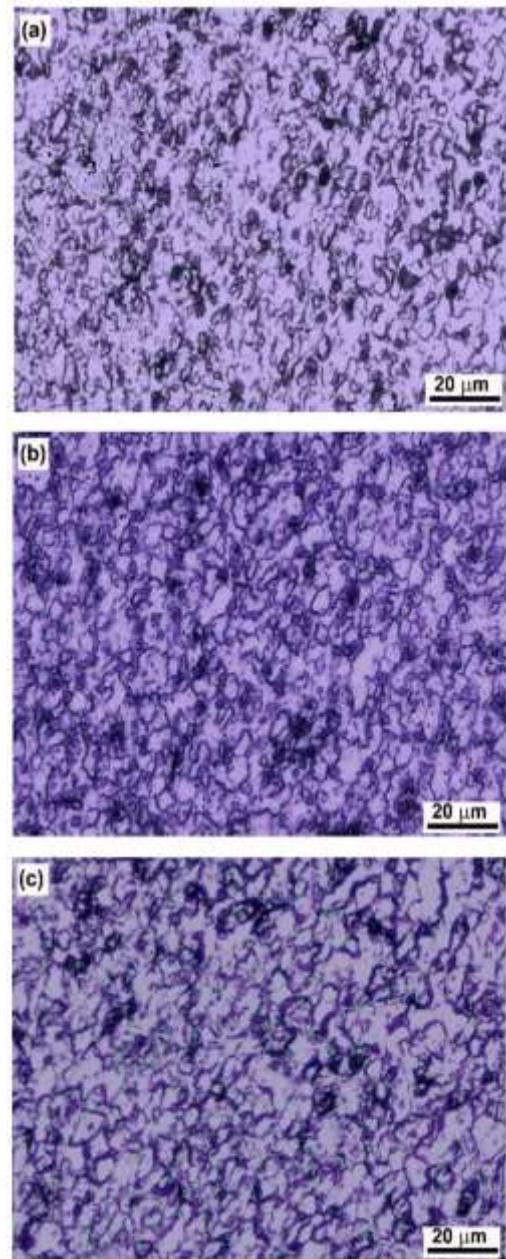


Figure 14. SZ microstructure of FSSW welded used a cylindrical pin in different RS: (a) 900 rpm (b) 1400 rpm (c) 1800 rpm

precipitation in SZ followed by continuous decrease along TMAZ and HAZ and the hardness values tend to constant at the BM as reported previously [9, 33]. However, they are different in terms of the magnitude of hardness, especially in the bottom of the exit hole due to variations in pin geometry and rotational speed.

In the FSSW joint produced using a cylindrical pin, the hardness curve in the upper sheet is higher than that measured in the lower sheet especially along the HAZ region but such a significant difference is not observed in

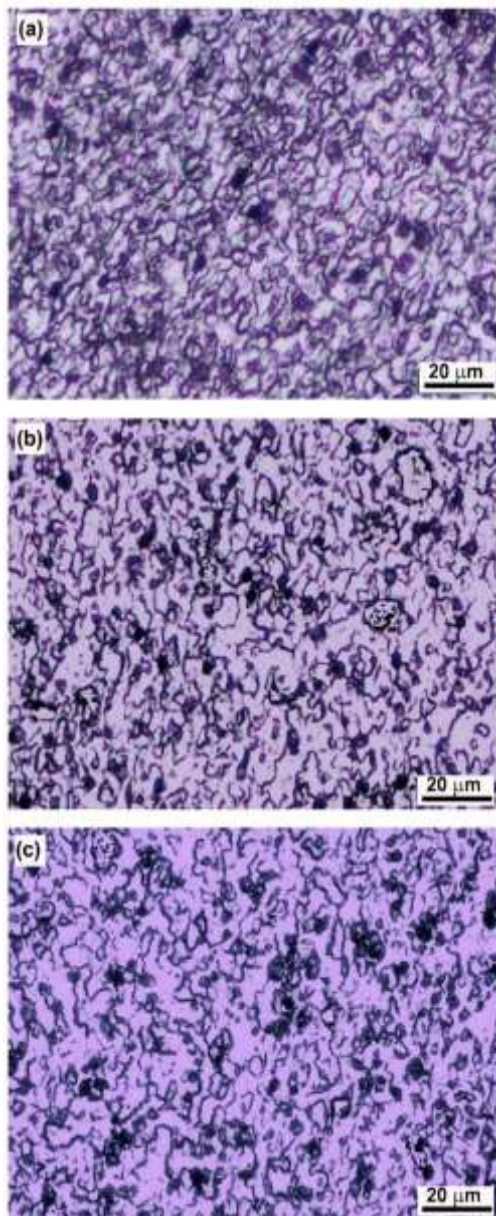


Figure 15. SZ microstructure of FSSW welded used a step pin in different RS: (a) 900 rpm (b) 1400 rpm (c) 1800 rpm

the FSSW joints produced using step pin. It is interesting to note that at the bottom of the keyhole, a continuous decrease in the hardness is observed with increasing tool rotational speed, especially in FSSW prepared using step pin. It may be argued that the use of step pin produced more heat which results in coarsening the precipitates hence softening [21, 34, 35].

3. 4. Strengths The maximum shear loads of the FSSW AA2024-O joints welded using different pin geometry and rotational speeds are shown in Figure 18. The maximum shear loads of FSSW joints that use

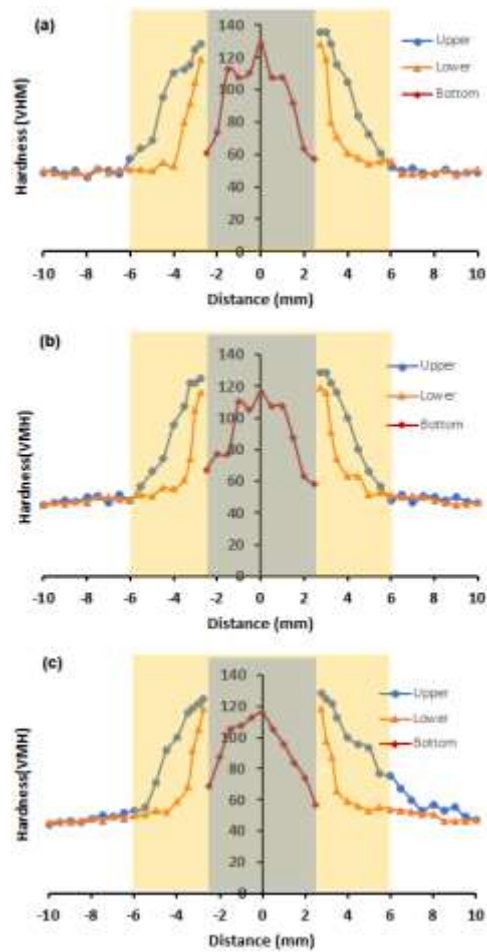


Figure 16. Microhardness distribution in a cross-section of FSSW welds used a cylindrical pin in different RS: (a) 900 rpm (b) 1400 rpm (c) 1800 rpm

cylindrical pin increase with increasing rotational speed until the highest value of the maximum shear load is achieved at 1400 rpm. On further increase in the rotational speed to 1800 rpm, the shear load decrease. Similar behaviors are observed in the FSSW joints produced using a step pin but with the lower magnitudes over a wide range of tool rotational speed, typically between 900-1800 rpm.

The strengths of the FSSW joints are determined by the structure of the welds, i.e. the FBR length and grain size in the SZ area [36].

The formation of FBR and grain size in SZ are influenced by the heat input which in turn tool rotational speed and pin geometry. The higher rotational speeds produce the higher strain and heat input making a wider FBR. Subsequently, the wider FBR results in a higher maximum fracture load. On the other hand, the strength of metallic materials including aluminum welded joints is controlled by grain size according to Hall-Petch as given by Mathers [37].

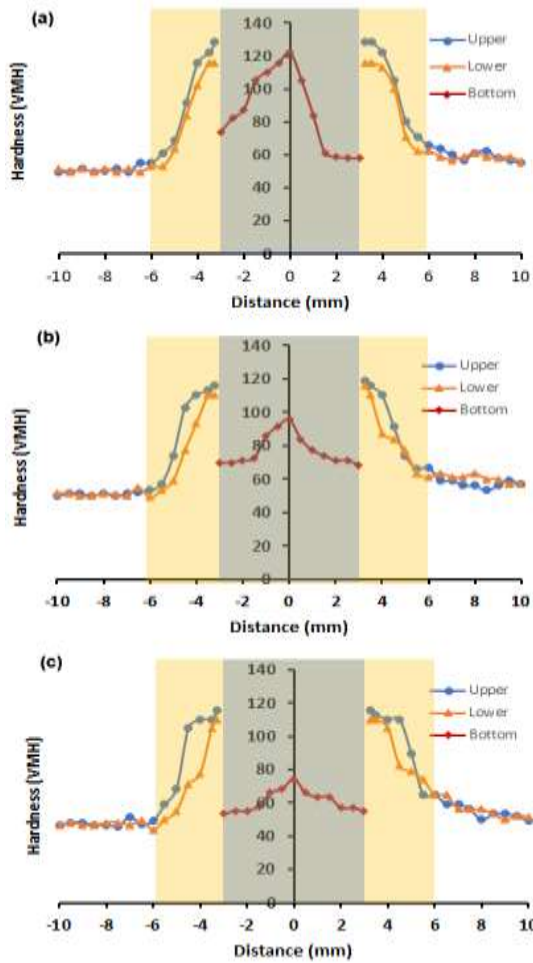


Figure 17. Microhardness distribution in a cross-section of FSSW welds used a step pin in different RS: (a) 900 rpm (b) 1400 rpm (c) 1800 rpm

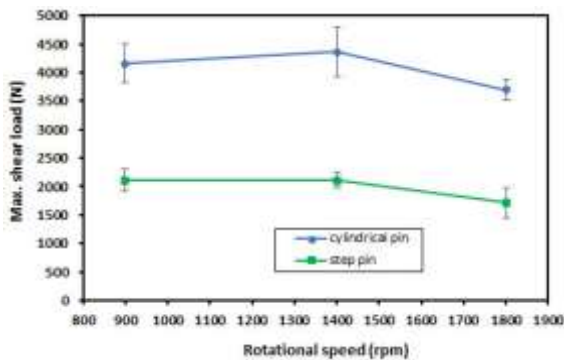


Figure 18. Maximum shear load in pin geometry and rotational speed tool variation

$$\sigma_y = \sigma_l + k_y d^{-\frac{1}{2}} \quad (2)$$

where d is the average diameter of the grains while σ_l and k_y are constants. It seems that increasing heat input due to

increased tool rotational has two conflicting effects. On one hand, high heat input increases the FBR length hence increasing the strength but it also causes coarsening of the microstructure resulting in reduced strengths. Therefore, the optimum tool rotational speed for both cylindrical and step pins seems to be achieved at the rotational speed of 1400 rpm owing to the balanced between these two factors.

Figures 19 and 20 show fractured surfaces of the FSSW joints under applied shear loads. It can be seen that

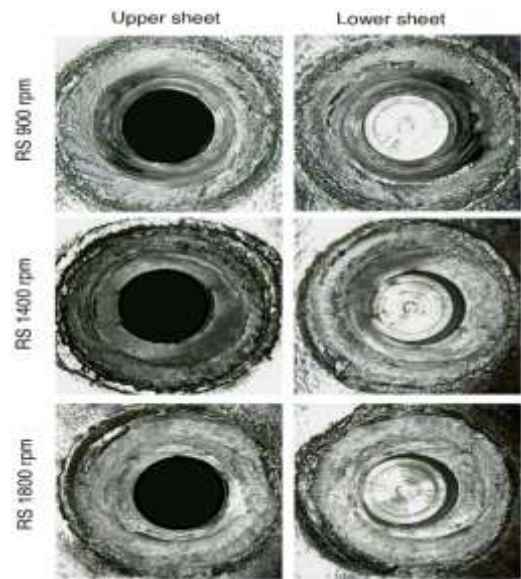


Figure 19. Fracture surfaces of FSSW joints under shear load using a cylindrical pin at different RS

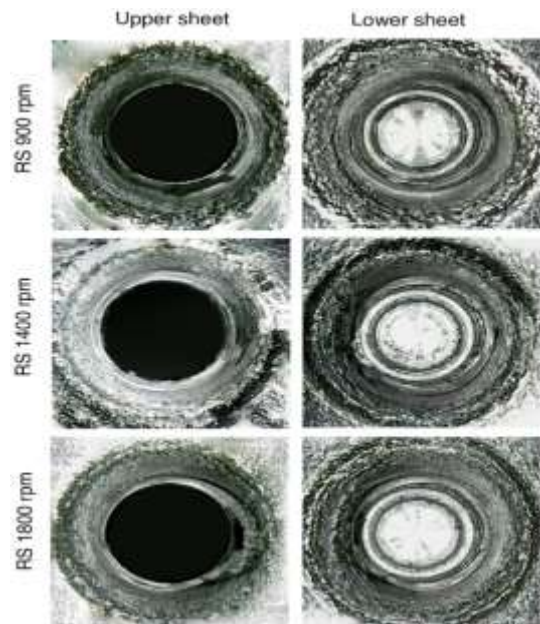


Figure 20. Fracture surfaces of FSSW joints under shear load using a step pin at different RS

at low tool rotational speed, typically of 900 rpm, the weld joints prepared using both cylindrical and step pins reveal failures correspond to shear mode. The failures are initiated by the formation of cracks at the hook tips which have high-stress concentrations. The cracks then propagate circumferentially along the stir zone (SZ) leading to final failure. At higher tool rotational speed, typically 1400 rpm or above, the failure mode change from shear to pullout in the nugget zone. The plausible explanation can be seen in Figure 21. As previously discussed, increasing tool rotational speed increases heat input and makes FBR wider. As a result, the working shear stress at the SZ under applied shear loads becomes lower so that the weakest part of the FSSW joints moves to the circumferential plane at the hook tip parallel to the exit hole. This condition combined with the moment of a couple due to eccentricity (misalignment) of the applied loads in the lap joints can cause nugget pullout.

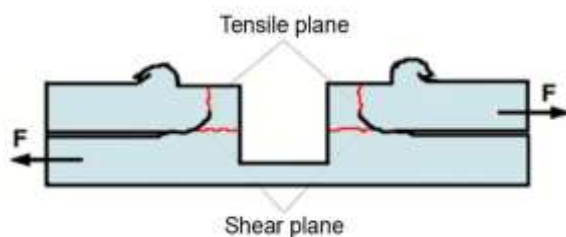


Figure 21. Schematic illustration of shear and tensile stresses around the SZ under applied shear stress

4. CONCLUSIONS

In this study, the effects of pin geometry and tool rotational speed on temperature profiles, microstructure, and mechanical properties of the FSSW joints aluminum alloy AA2024-O have been investigated and the following conclusions are drawn :

- Heat generated by the FSSW process is determined by the pin geometry and tool rotational speed. The tool has a step pin that produces more heat compared to the cylindrical pin due to the more frictional area in the step pin.
- The SZ region has the highest hardness probably due to re-precipitation then the hardness continuously decreases across TMAZ/HAZ and finally becomes constant along with BM.
- For the FSSW joints prepared using both cylindrical and step pins, the highest value of the maximum shear load is achieved at the tool rotational speed of 1400 rpm. It seems that this optimum tool rotational speed produces a proper combination of FBR length and grain size with the failure mode showing pullout nuggets.

5. REFERENCES

1. Rambabu P., N. Eswara Prasad, N.E., V.V. Kutumbarao, V.V., Wanhill, R.J.H., "Aluminium Alloys for Aerospace Applications", Aerospace Materials and Material Technologies, Indian Institute of Metals Series, Springer Science+Business Media Singapore, (2017). DOI: 10.1007/978-981-10-2134-3.
2. Rajan, R., Kah, P., Mvola, B., Martikainen, J., "Trends in Aluminium Alloy Development and their Joining Methods", *Annual Review of Material Science*, Vol. 44, (2015), 383-397.
3. Kaushik, N., Singhal, S., "Experimental Investigations on Microstructural and Mechanical Behavior of Friction Stir Welded Aluminum Matrix Composite", *International Journal of Engineering, Transactions A: Basics*, Vol. 32, No. 1, (2019), 162-170. DOI: 10.5829/ije.2019.32.01a.21.
4. Thomas, W.M., "Friction stir welding and related friction process characteristics", Inalco, International conference joint in aluminium Cambridge, UK., (1998).
5. Karthikeyan, R., Balasubramanian, V., "Predictions of the optimized friction stir spot welding process parameters for joining AA2024 aluminum alloy using RSM", *International Journal of Advanced Manufacturing Technology*, Vol. 51, No. 1-4, (2010), 173-183. DOI: 10.1007/s00170-010-2618-2.
6. Song, X., Ke, L., Xing, L., Liu, F., Huang, C., "Effect of plunge speeds on hook geometries and mechanical properties in friction stir spot welding of A6061-T6 sheets", *International Journal of Advanced Manufacturing Technology*, Vol. 71, No. 9-12, (2014), 2003-2010. DOI: 10.1007/s00170-014-5632-y
7. Khatami, H., Azdast, T., Mojaver, M., Hasanzadeh, R., Rafiei, A., "Study of Friction Stir Spot Welding of Aluminum/Copper Dissimilar Sheets using Taguchi Approach", *International Journal of Engineering, Transactions B: Applications*, Vol. 34, No. 05, (2021), 1329-1335. DOI: 10.5829/ije.2021.34.05b.28
8. Sprovieri, Jhon, "Friction Stir Spot Welding", *Assembly Magazine*, (2016), 1-6. <http://www.assemblymag.com/articles/93337>
9. Paidar, M., Sadeghi, F., Najafi, H., Khodabandeh, A. R., "Effect of Pin and Shoulder Geometry on Stir Zone and Mechanical Properties of Friction Stir Spot-Welded Aluminum Alloy 2024-T3 Sheets", *Journal of Engineering Materials and Technology*, Vol. 137, No. 031004, (2015), 1-6. DOI: 10.1115/1.4030197.
10. Badarinarayan, H., Yang, Q., Zhu, S., "Effect of tool geometry on static strength of friction stir spot-welded aluminum alloy", *International Journal of Machine Tools & Manufacture*, Vol. 49, (2009), 142-148. DOI: 10.1016/j.ijmactools.2009.06.001.
11. Enami, M., Farahani, M., Farhang, M. "Novel study on keyhole less friction stir spot welding of Al 2024 reinforced with alumina nanopowder.", *The International Journal of Advanced Manufacturing Technology*, Vol. 101, (2019), 3093-3106. DOI: 10.1007/s00170-018-3142-z
12. Klobcar, D., Tu, J., Smolej, A., Simon, S., "Parametric study of FSSW of aluminium alloy 5754 using a pinless tool", *Weld World*, Vol. 59, (2015), 269-281. DOI: 10.1007/s40194-014-0208-x
13. Baek, S., Choi, D., Lee, C., Ahn, B., Yeon, Y., Song, K., Jung, S., "Microstructure and Mechanical Properties of Friction Stir Spot Welded Galvanized Steel", *Materials Transactions*, Vol. 51, No. 5, (2010), 1044-1050. DOI: 10.2320/matertrans.M2009337.
14. Baskoro, A.S., Hadisiswojo, S., Kiswanto, G., Winarto, Amat, M.A., Chen, Z.W. "Influence of welding parameters on macrostructural and thermomechanical properties in micro friction stir spot welded under high-speed tool rotation.", *The International Journal of Advanced Manufacturing Technology*, Vol. 106, (2020), 163-175. DOI:10.1007/s00170-018-3142-z.
15. Alheta, S., Zayan, S., Mahmoud, T., Gomaa, A., "Optimization of Friction Stir Spot Welding Process Parameters for AA6061-T4

- Aluminium Alloy Plates”, *American Scientific Research Journal for Engineering, Technology, and Sciences (ASRJETS)*, Vol. 20, (2016), 244-253.
16. Miles, M., Karki, U., Hovanski, Y., “Temperature and Material Flow Prediction in Friction-Stir Spot Welding of Advanced High-Strength Steel”, *JOM*, Vol. 66, No. 10, (2014), 2130-2136. DOI: 10.1007/s11837-014-1125-6
 17. D’Urso, G., “Thermo-mechanical characterization of friction stir spot welded AA6060 sheets: Experimental and FEM analysis”, *Journal of Manufacturing Processes*, Vol. 17, (2015), 108-119. DOI: 10.1016/j.jmapro.2014.08.004
 18. Chen, K., Liu, X., Ni, J., “Effects of Process Parameters on Friction Stir Spot Welding of Aluminum Alloy to Advanced High-Strength Steel”, *Journal of Manufacturing Science and Engineering*, Vol. 139, No. 8, (2017) 81016-1-9. DOI: 10.1115/1.4036225.
 19. Tiwan, Ilman, M.N., Kusmono, “Microstructure and mechanical properties of friction stir spot welded AA5052-H112 aluminum alloy”, *Heliyon*, Vol. 7, (2021), e06009. DOI: 10.1016/j.heliyon.2021.e06009
 20. Shekhawat, R.S., Nadakuduru, V.N., Nagumothu, K.B., “Microstructures and mechanical properties of friction stir spot welded Al 6061 alloy lap joint welded in air and water”, *Materials Today: Proceedings*, Vol. 41, (2021), 995-1000. DOI: 10.1016/j.matpr.2020.06.065.
 21. Ethiraj, N., Sivabalan, T., Sivakumar, B., Vignesh Amar, S., Vengadeswaran, N., Vetrivel, K., “Effect of Tool Rotational Speed on the *Tensile* and Microstructural Properties of Friction Stir Welded Different Grades of Stainless Steel Joints”, *International Journal of Engineering, Transactions A: Basics*, Vol. 33, No. 1, (2020), 141-147. DOI: 10.5829/ije.2020.33.01a.16
 22. Kim, J., Ahn, E., Das, H., Jeong, Y., Hong, S., Miles, M., Lee, K., “Effect of Tool Geometry and Process Parameters on Mechanical Properties of Friction Stir Spot Welded Dissimilar Aluminum Alloys”, *International Journal of Precision Engineering and Manufacturing*, Vol. 18, No. 3, (2017), 445-452. DOI: 10.1007/s12541-017-0053-0.
 23. Schmidt H., J. Hattel, J. Wert, “An analytical model for the heat generation in friction stir welding”, *Modelling and Simulation in Materials Science and Engineering*, Vol. 12, No. 1, (2004), 143-157. DOI: 10.1088/0965-0393/12/1/013
 24. Mijajlovic, M., Milcic, D., “Analytical Model for Estimating the Amount of Heat Generated During Friction Stir Welding: Application of plates Made of Aluminium Alloy 2024 T351”, *InTech, Welding Processes*, 247-274, (2012). DOI: 10.5772/53563
 25. Babu, S., Sankar, V. S., Ram, G. D. J., Venkitakrishnan, P. V., Reddy, G. M., Rao, K. P., “Microstructures and Mechanical Properties of Friction Stir Spot Welded Aluminum Alloy AA201”, *Journal of Materials Engineering and Performance*, Vol. 22, (2013), 71-84. DOI: 10.1007/s11665-012-0218-z
 26. Yang, Q., Mironov, S., Sato, Y. S., Okamoto, K., “Material flow during friction stir spot welding”, *Materials Science and Engineering A*, Vol. 527, No.16-17, (2010), 4389-4398. DOI: 10.1016/j.msea.2010.03.082
 27. Shen, Z., Yang, X., Zhang, Z., Cui, L., Yin, Y., “Mechanical properties and failure mechanisms of friction stir spot welds of AA 6061-T4 sheets”, *Materials and Design*, Vol. 49, (2013), 181-191. DOI: 10.1016/j.matdes.2013.01.066
 28. Mahmoud, T. S., Khalifa, T. A., “Microstructural and mechanical characteristics of aluminum alloy AA5754 friction stir spot welds”, *Journal of Materials Engineering and Performance*, Vol. 23, No. 3, (2014), 898-905. DOI: 10.1007/s11665-013-0828-0.
 29. Mishra, R.S., Ma, Z.Y., “Friction Stir Welding and Processing”, *Material Science and Engineering R: Reports*, Vol. 50, No. 1-2, (2005), 1-78. DOI: 10.1016/j.mser.2005.07.001
 30. Pathak, N., Bandyopadhyay, K., Sarangi, M., Panda, S. K., “Microstructure and Mechanical Performance of Friction Stir Spot-Welded Aluminum-5754 Sheets”, *Journal of Materials Engineering and Performance*, Vol. 22, No. 1, (2013), 131-144. DOI: 10.1007/s11665-012-0244-x
 31. Zhou, L., Luo, L. Y., Zhang, T. P., He, W. X., Huang, Y. X., Feng, J. C., “Effect of rotation speed on microstructure and mechanical properties of refill friction stir spot welded 6061-T6 aluminum alloy”, *International Journal of Advanced Manufacturing Technology*, Vol. 92, No. 9-12, (2017), 3425-3433. DOI: 10.1007/s00170-017-0359-1
 32. Li, Z., Gao, S., Ji, S., Yue, Y., Chai, P., “Effect of Rotational Speed on Microstructure and Mechanical Properties of Refill Friction Stir Spot Welded 2024 Al Alloy”, *Journal of Materials Engineering and Performance*, Vol. 25, No. 4, (2016), 1673-1682. DOI: 10.1007/s11665-016-1999-2
 33. Ji, S., Li, Z., “Microstructure and Mechanical Properties of Friction Stir Lap Welded Mg / Al Joint Assisted by Stationary Shoulder”, *Metals and Materials International*, Vol. 23, No. 6, (2017), 1158-1167. DOI: 10.1007/s12540-017-7065-2
 34. Chen, Y., Ding, H., Li, J., Zhao, J., Fu, M., Li, X., “Effect of welding heat input and post-welded heat treatment on hardness of stir zone for friction stir-welded 2024-T3 aluminum alloy”, *Transactions of Nonferrous Metals Society of China*, Vol. 25, No. 8, (2015), 2524-2532. DOI: 10.1016/S1003-6326(15)63871-7
 35. Sonne, M. R., Tutum, C. C., Hattel, J. H., Simar, A., De Meester, B., “The effect of hardening laws and thermal softening on modeling residual stresses in FSW of aluminum alloy 2024-T3”, *Journal of Materials Processing Technology*, Vol. 213, No. 3, (2013), 477-486. DOI: 10.1016/j.jmatprotec.2012.11.001
 36. Zhou, L., Zhang, R. X., Li, G. H., Zhou, W. L., Huang, Y. X., Song, X. G., “Effect of pin profile on microstructure and mechanical properties of friction stir spot welded Al-Cu dissimilar metals”, *Journal of Manufacturing Processes*, Vol. 36, No. 7, (2018), 1-9. DOI: 10.1016/j.jmapro.2018.09.017
 37. Mathers, Gene, “The welding of aluminium and its alloys,” First published, Woodhead Publishing Ltd and CRC Press LLC, (2002).

Persian Abstract

چکیده

در مطالعه حاضر، اثر هندسه پین و سرعت چرخش ابزار بر ریزساختار و مشخصات مکانیکی اتصال AA2024-O FSSW بررسی شد. از دو نوع هندسه پین متفاوت، یعنی پایه های استوانه ای و پله ای و سه سرعت چرخش متفاوت 1400، 900 و 1800 دور در دقیقه در اتصال جوشکاری نقطه اصطکاک استفاده شده است. مشاهده ریزساختار، اندازه گیری سختی و آزمایش برشی انجام شد. نتایج نشان می دهد که هندسه پین و سرعت چرخش تأثیر قابل توجهی بر ریزساختار و حداکثر بار برشی اتصالات جوش دارند. برای هر دو هندسه پین، با افزایش سرعت چرخش، ارتفاع و عرض قلاب منطقه کاملاً باند شده (FBR) افزایش می یابد. اتصال جوش توسط یک پین استوانه ای تولید می شود که مقادیر بیشتری از ارتفاع و عرض قلاب FBR نسبت به استفاده از پایه پله ای نشان می دهد. بعلاوه، بالاترین مقدار در حداکثر بار برشی با سرعت چرخش 1400 دور در دقیقه برای هر دو پایه استوانه ای و پله ای بدست می آید. یافته دیگر این است که حداکثر بارهای برشی اتصالات FSSW تولید شده با یک پین استوانه ای بیشتر از آن است که با استفاده از پین استپ ساخته شده است.
